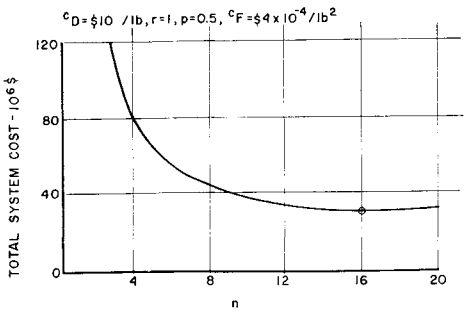

Fig. 3 Example of variation in total system cost with number of launchings including development costs.

of curve A ($p = 0.8$) with curve C in Fig. 1 shows that the optimum n decreases as p decreases; of course, when p and c_F become very small for a developed system, a single launch by a large booster will be best (curve E). Figure 2 also shows the variation of vehicle gross weight with number of launches for both $p = 0.5$ and $p = 0.8$. Comparison of these curves shows that if 5 launches (near minimum cost) were used at $p = 0.5$, 8 launches would be required to put the same total payload up with $p = 0.8$.

Figures 1 and 2 assumed no development cost. If a development cost c_D = \$1000/lb (with $r = 1.0$) is added to the other conditions represented by curve C of Fig. 1, the curve of Fig. 3 results. The optimum number of launches has tripled, from 5 in Fig. 1 to 16 in Fig. 3. Of course, the effect would be smaller for r somewhat less than unity (which would probably be more realistic), and furthermore, r should tend to decrease as n goes up (due to mass production benefits), so that the sample comparison is somewhat exaggerated.

Concluding Remarks

These simple examples have indicated that under certain conditions it would be better to boost a given payload into space by dividing it into several parts boosted separately, as one might have expected. Of course, only launch-system costs have been considered here; if mission constraints for manned vehicles (e.g., for re-supply missions) were imposed, there would probably be more distinct limits on n. Further, for payloads to be assembled in space, there could arise a weight penalty for assembly problems at large n. Finally, for manned missions, a very low failure probability p will necessarily be sought; this leads to low n_{opt}. However, it remains that a rather simple analysis might be used to assess the importance of various factors on optimum vehicle size for multiple launchings to put a given total payload into space, or for providing a multi-purpose spacecraft booster system.

Elastomeric Seals in Hard Vacuum

TED R. CARRELL* AND HAROLD BLAIR†
Parker Seal Company, Culver City, Calif.

EFFECTIVE sealing against the "hard" vacuum of interplanetary space has been one of the problems facing designers of advanced vehicles. At first, use of elastomeric (rubber) seals in space applications seemed limited, since early studies indicated that hard vacuums would cause conventional elastomers to volatilize and evaporate.

Received February 13, 1963; revision received October 25, 1963.

* Manager, Engineering Services.
† Chief Engineer, Development.

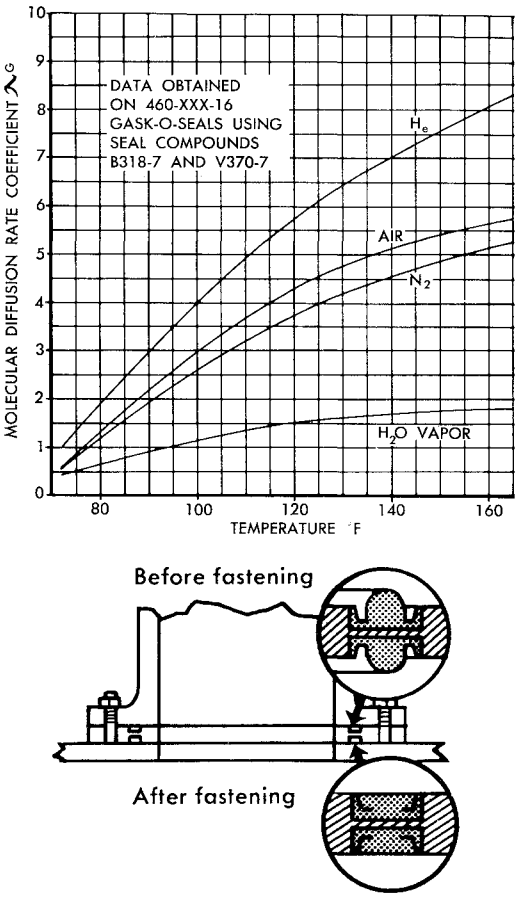

Fig. 1 Vacuum molecular diffusion rate coefficient of various gases as a function of temperature.

However, assuming that better elastomeric polymers and special seal designs might change the viewpoint toward elastomers, the authors conducted a test program to provide data on hard vacuum elastomeric seals for specific space projects. The results indicate a much greater design flexibility for engineers in the application of elastomer seals for vacuum than was generally supposed, and the possibility of a mathematical formula for determining leak rates of various gases with such seals.

Hard vacuum (vacuums below the level of 10^{-6} mm Hg, torr) affects elastomeric materials in two general ways. First, evaporation of the material or of a volatile component of the material may occur. Second, high vacuum may cause alteration of the seal structure affecting its mechanical characteristics and other physical properties. The rates of these reactions can be radically affected by thermal extremes.

However, a research program had already provided data showing that, although certain rubbers volatilize rapidly from 10^{-7} to 10^{-8}, a specially formulated elastomeric material was unaffected at vacuums of 10^{-9} torr.[1]

There was also evidence to support the supposition that the percentage of weight loss depends on geometry, for only those monomers at the surface were removed. Studies performed on meteorites verify the concept of progressive surface decomposition of macromolecules of polymeric materials in hard vacuums. This indicated that careful design of seal geometry might help minimize vacuum erosion.

The program was based on the use of specially compounded seal materials in a "controlled confinement" (Gask-O-Seal)‡ design configuration. This type of seal has been widely used for many years in aircraft and missile applications. Basically, it is a grooved metal retainer containing a molded-in-place special-configuration rubber seal element. Typical

‡ Parker Seal Company Trademark.

of it is the closely controlled confinement of a specially compounded rubber sealing element and the limited area of seal exposure to the fluid or gas being sealed.

Its design was chosen because the ratio of the controlled high-rubber volume to the groove void in this design prevents movement of the seal (see Fig. 1).

The use of seal materials with low vapor pressures was desirable, but there were other considerations. Silicone rubber has a very low vapor pressure but has a permeability about 100 times greater than Butyl. One seal material selected for testing was a Butyl elastomer compound B318-7 that was developed for use in hermetic sealing applications. In addition, special high-temperature Viton compounds were devised, designated V370-7 and 77-545.

In one series of tests, the following objectives were outlined. Weighed, microtomed slice samples of B318-7 and V370-7 were to be held in the pressure range of 10^{-8} torr at various temperatures to determine weight loss and were subsequently to be examined microscopically for evidence of deterioration.

A test system was devised using vacuum pumping equipment consisting of a fore-pump, a two-stage mercury diffusion pump, and an ion gettering pump that were connected in series. The system was roughed down to a vacuum of approximately 2×10^{-4} torr, using the first two pumping units, and the ion pump power supply was turned on. After pumping of the ion pump system was established, the glass lead to the roughing system was fused off. When the system pressure reached 1.5×10^{-7} torr, the heating elements were turned on and adjusted to achieve the test temperature. Under continuous ion pumping, the samples were maintained at this test temperature for 8 days at a stabilized pressure level of 1.2 to 6×10^{-8} torr.

The microtomed samples experienced weight loss at the specific temperatures given in Table 1. Microscopic

Table 1 Weight loss under vacuum as a function of temperature

Compound	Temperature, °F	Weight loss, %	Pressure, torr
B318-7, Butyl base	77	3.3	6×10^{-8}
	120	5.1	2×10^{-8}
	165	6.8	3×10^{-8}
V370-7, Fluoroelastomer base	77	0	1.2×10^{-8}
	120	0.7	4×10^{-8}
	165	1.3	5×10^{-8}
77-545,[a] Fluoroelastomer base	77	2.1	1.8×10^{-9}
E-515-8,[b] Ethyl Propylene base	75	0.4	4×10^{-8}

Separate sets of samples were tested at each temperature:
[a] Duration of test—84 hrs.
[b] Duration of test—24 days.

examination under 50, 100, and 200 times magnification showed no surface deterioration of any of the samples tested. The very slight weight loss was attributed to the removal of simple volatiles, primarily water vapor, from the elastomer. Once this had been shown, the next step was to determine molecular diffusion rates (leak rates) of the "controlled confinement" seal containing these seal elastomers.

(The term "molecular diffusion rate," as used here, refers to the net transfer of gas from one side of a seal member to the other. This definition does not include outgassing or leakage that might occur from a purely mechanical standpoint due to errors in assembly, improper design, seal damage, etc.)

Of course, in dealing with extremely small leaks of a molecular nature, the interval of time needed to reach a decision about the actual occurrence of a leak becomes quite large. In addition, when determining the actual molecular diffusion rate, it is always necessary to distinguish between the evolution of gas due to outgassing in the system itself, which is transient, and gas load due to diffusion, which should stabilize. The rate of evolution due to outgassing will, in general, decrease with time and should ultimately become extremely small, whereas molecular diffusion after stabilization should remain constant with time at a given temperature and pressure level.

The seals for the molecular diffusion rate tests were installed in test fixtures and connected to a CEC 24-120B mass spectrometer helium leak detection instrument. Complete helium leak rate stabilization was achieved for each test for room temperature operation.

This test series established that the molecular diffusion rates of helium at 72°F for the seal containing B318-7 elastomer are within a range of 0.5–0.7 atm cm³/in. of seal per year. The corresponding range for 77-545 elastomer is from 1.0–3.0 atm cm³ He/in./yr. An additional test series evaluating E515-8 elastomer gave a value of 3.0 atm cm³ He/in./yr for this material at a pressure of 1×10^{-5} torr.

Molecular diffusion rate coefficients of the seal for different gases at various temperatures were obtained to determine if data on helium could be connected to other gases by a mathematical formula rather than by testing each gas.

Pressure decay measurements were taken by measuring the pressure rise in the closed system over a 3-hr period at the specified test temperature on several gases. Each test was conducted three times before changing the experimental conditions. The original test seal was then replaced by another Gask-O-Seal, and the experimental procedure repeated with the next gas to be evaluated.

The pressure decay data from the tests have been reduced to the molecular diffusion rate coefficient curves of Fig. 1. These curves check quite accurately with a theoretical treatment of the prediction of a change in permeability velocity of a gas based on calculations of the molecular diameter of the gas and the extent of the electron cloud about the gas molecule.

Thus, it appears that an equation can be established relating the molecular diffusion rates of specific gases to the diffusion rates determined using a test gas based on these curves. This equation is

$$Q_2 = Q_1[(\lambda G)/_2(\lambda G)_1]$$

where

Q = molecular diffusion rate
λG = molecular diffusion rate coefficient
1 = test gas of known diffusion rate at a known temperature
2 = test gas for which diffusion rate is to be calculated for temperatures 72°–165°F

As an example, note the nitrogen molecular diffusion rate of the seal with 77-545 as the seal element at 160°F. $(\lambda G)_2 = 5.1$ is 3.4 atm cc N_2/in./yr if its helium diffusion rate is determined as 1.2 atm cm³ He/in./yr at 79°F; $(\lambda G)_1 = 1.8$.

The tests also indicated that the "controlled confinement" design seal can work well at pressure as low as 2×10^{-9} torr. In fact, since this pressure was at the limit of the pumping system capability with no appreciable effect on the seal material, one may expect that the seals developed will withstand pressure levels even lower than 10^{-9} mm Hg.

Perhaps equally important as the sealing properties of such seals was their demonstrated reusability and the interchangeability of the parts. This could eliminate many maintenance problems resulting from soldering, welding, and other similar types of sealing often used on hard vacuum equipment.

We look forward to extending the range of reusable seals to more rigorous vacuum applications as new seal materials are discovered and perfected.

Reference

[1] Hayes, R. A., Smith, F. M., Smith, W. A., and Kitchen, L. J., "Islinger's papers in proceedings of Illuminating Engineering Society," Wright Air Dev. Center TR 56-331 (1959).

Design Guides for Tapered Transition Sections for Pressure Vessels

I. W. DINGWELL*
Arthur D. Little, Inc., Cambridge, Mass.

Tapered transition sections to generate constant strength (and thus minimum weight) design criteria for symmetrically loaded thin shells of revolution are analyzed. A finite difference solution (digital computer) to Love's first approximate thin-shell theory is used. Tapered transition sections are considered for a cylindrical pressure vessel (R/t = 100) closed by either hemispherical, torispherical, or 2:1 ellipsoidal heads.

Introduction

AT the juncture of two dissimilar shells, shear and bending moments arise which raise the stress level above the desired membrane stress. A correctly designed transition section will minimize the effects of these discontinuity forces and moments, and a shell structure will result that has nearly constant strength. If the design or membrane stress level is close to the yield point of the material, then a minimum weight design will result. The present study determines the dimensions of tapered transition sections at the junctures of various heads with the main cylindrical wall of a minimum weight pressure vessel.

The normal method[1] of solving the juncture problem is to generate the "edge influence coefficients" of each of the shells and solve the equilibrium and compatibility equations for the forces and moments at the juncture. For instance, the variation of the meridional bending moment in a spherical cap near a boundary is

$$M_\phi = -t(C_2 \cos\beta + C_1 \sin\beta)e^{-\beta} \qquad (1)$$

where t is the shell thickness, C_1 and C_2 are constant coefficients related to edge loads and shell geometry, and $\beta = S/(2R_\theta t)^{1/2}$, where R_θ is the radius of curvature in the circumferential direction, and S the surface length from boundary.

Evaluation of Eq. (1) indicates that the applied edge moment is reduced to less than 10% of its original value when $\beta \sim 2$, or $S \sim 3(R_\theta t)^{1/2}$. The so-called characteristic length $(R_\theta t)^{1/2}$ is extremely important in the design of tapered transition sections because the membrane stress condition will predominate in little more than three characteristic lengths from a boundary. In a spherical cap, this fixes the maximum length of the transition section.

By means of a digital computer solution[2] based on the linear theory of symmetrically loaded thin shells of revolution (Love's first approximation with small displacements), one can calculate the edge influence coefficients and solve the juncture problem. The computer analysis will generate directly the forces, moments, displacements, and rotations at the juncture. In this note, tapered transition sections are examined for three kinds of shell junctures (Figs. 1–3), and several tapers are considered for each. In all cases, the cylindrical section has a radius/thickness ratio of 100. The heads are selected on a rough basis of equal weight, with radius-of-curvature/thickness ratios of the order 200. These dimensions fall within the range that may be analyzed by linear elastic thin-shell theory (i.e., $500 > R/t > 50$).

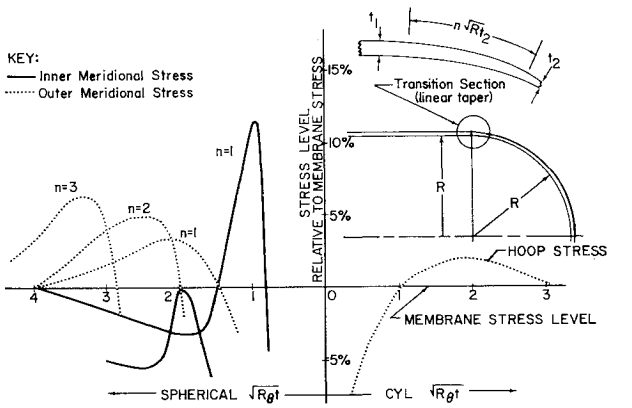

Fig. 1 Stresses at the juncture of a hemispherical head and cylinder with linear taper in transition section.

Hemispherical Head-Cylinder Junctures (Fig. 1)

Constant strength design would dictate that the thickness of the head be one-half the thickness of the cylinder. Discontinuity stresses will arise at the joint due to the differences in bending resistance and radial stiffness of the shell edges when the vessel is pressurized; hence bending moments and shear forces will be generated. For an abrupt joint (no taper), the maximum hoop stress in the head will be 7% above the membrane stress.

Figure 1 shows the maximum stresses in the head and cylinder with linearly tapered sections of length $n(R_\theta t)^{1/2}$, where n = 1, 2, and 3. For n = 1 (a linear taper which doubles the thickness of the shell in one characteristic length from the joint), the meridional stress on the inner surface is 11% higher than the membrane stress. As n is increased, this stress peak is reduced until the meridional stress on the outside surface begins to increase. The maximum stress in each taper occurs near or at the base of the taper in the head. A minimum stress, approximately 5% above membrane stress, is noted when n is between 1.5 and 2.

A taper was examined that was continuous in the first derivative. In that taper, the stress was further reduced to 4% above the membrane stress level. Thus for a cylindrical pressure vessel with hemispherical ends, the working stress level may be raised 3% by the use of tapered transition sections. This will effect a possible 3% reduction in weight.

Torispherical Head—Cylinder Junctures (Fig. 2)

Some torispherical head designs[3] appear to have slight weight advantages over the full hemispherical head. For the constant thickness, torispherical head with membrane-section stress equal to that of the cylindrical shell, the head thickness is 52.2% of the shell thickness. The torus-sphere juncture is 3 characteristic lengths away from the torus-cylinder juncture. Tapered transitions within the toroidal section (curves 1–3) lead to stresses 30–40% above membrane level. To reduce the stresses in this area, the full cylindrical thickness can be maintained through the toroidal sections, so that the tapered transition occurs in the spherical sector [curves E-1, E-2, and E-3, where the number signifies the value of n for the length of the linear taper, $n(R_\theta t)^{1/2}$]. The E-3 transition reduces the stress level to within 6% of the membrane stress level. (There is little to be gained in reducing the stress level further, because the maximum hoop stress in the cylindrical

Received March 26, 1963; revision received November 20, 1963.

* Senior Engineer.